The Abdus Salam International Centre for Theoretical Physics

United Nations Educational, Scientific and Cultural Organization

IAEA International Atomic Energy Agency

2359-17

Joint ICTP-IAEA Workshop on Physics of Radiation Effect and its Simulation for Non-Metallic Condensed Matter

13 - 24 August 2012

Applications of MD and long time scale techniques to radiation effects in oxide materials

Roger Smith

Loughborough University
United Kingdom

Applications of MD and long time scale techniques to radiation effects in oxide materials

Roger Smith
Loughborough University, UK.

Applications of the techniques

- High energy irradiation of MgO, $MgAl_2O_4$ and other spinels
- Fe with embedded yttria nanoparticles
- Magnetron sputter deposition of TiO_2 and ZnO

MgO

Substrates consisting of up to 190,000 atoms were investigated by MD.

Collision cascades initiated by imparting an energy to an atom somewhere in the centre of the system with energies from 400 eV to 5 keV.

Fixed charge potential model due to Lewis and Catlow splined to the ZBL for close interactions

Multipole method used for evaluating the Coulomb sums

Long time dynamics (TAD) used to evolve the defects left after the ballistic phase of the cascade.

Observation: Cascades in MgO are self similar over large areas

Di-interstitial recombination event for 400 eV O PKA

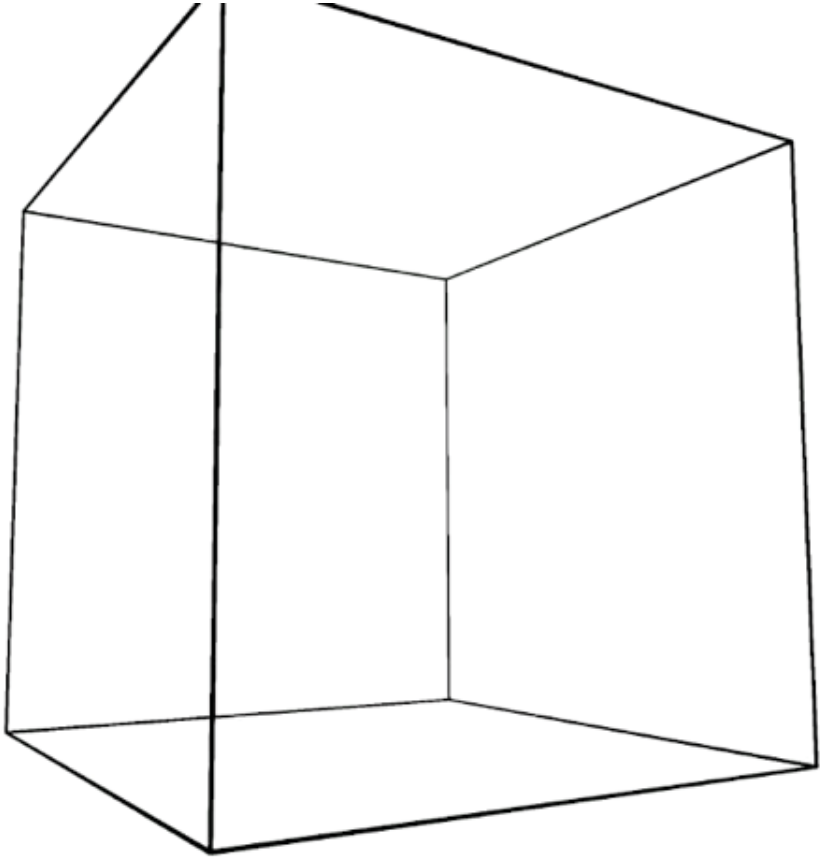

Colour Scheme

Large blue : Mg ion

Small light blue: Mg vacancy

Large red : O ion

Small light red : O vacancy

Peak damage 90 fs
Dimer forms 526 fs
Recombination starts 5330 fs

Examples from 5 keV cascades

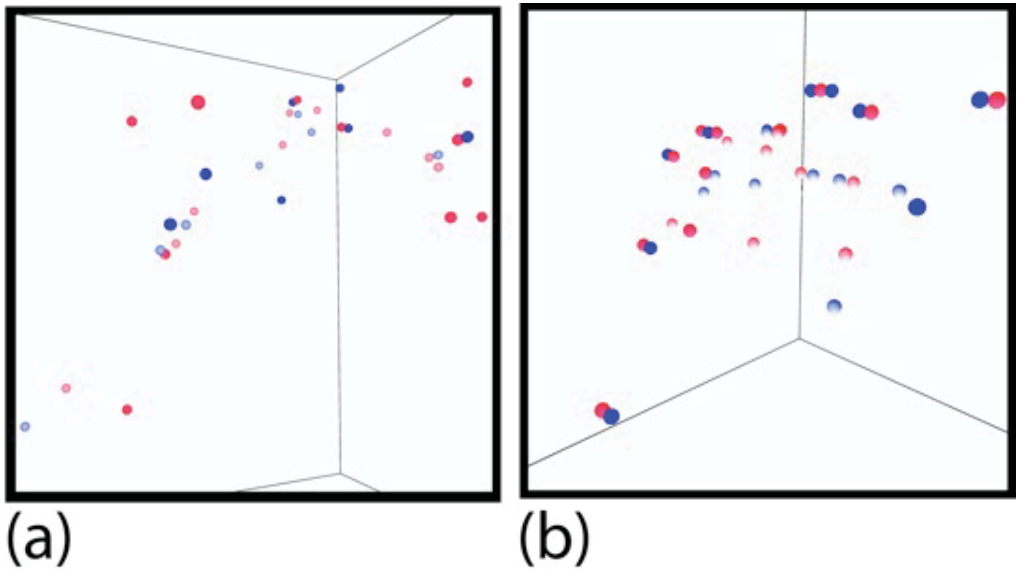

(a) 3 MgO dimers 2 vacancy dimers plus isolated interstitials (cube side 11.9 nm)
(b) 2 interstitial trimers, 4 dimers, 3 vacancy dimers.

Average number of defects observed in MgO after the collisional phase of the cascade

Energy (eV)	defect type			
	vacancy dimer	O interstitial	Mg interstitial	MgO dimer
400	0.05	0.15	0.05	0.15
2000	0.4	1.7	1.7	1.3
5000	1.3	4.8	5.2	3.3

At 5 keV a few interstitial trimers, one tetramer and one seven atom interstitial cluster also formed.
Statistics from 30 400 eV cascades; 12 cascades each at 2 and 5 keV.
Small relatively immobile defect clusters

Long time scale dynamics (TAD) of defect clusters in MgO

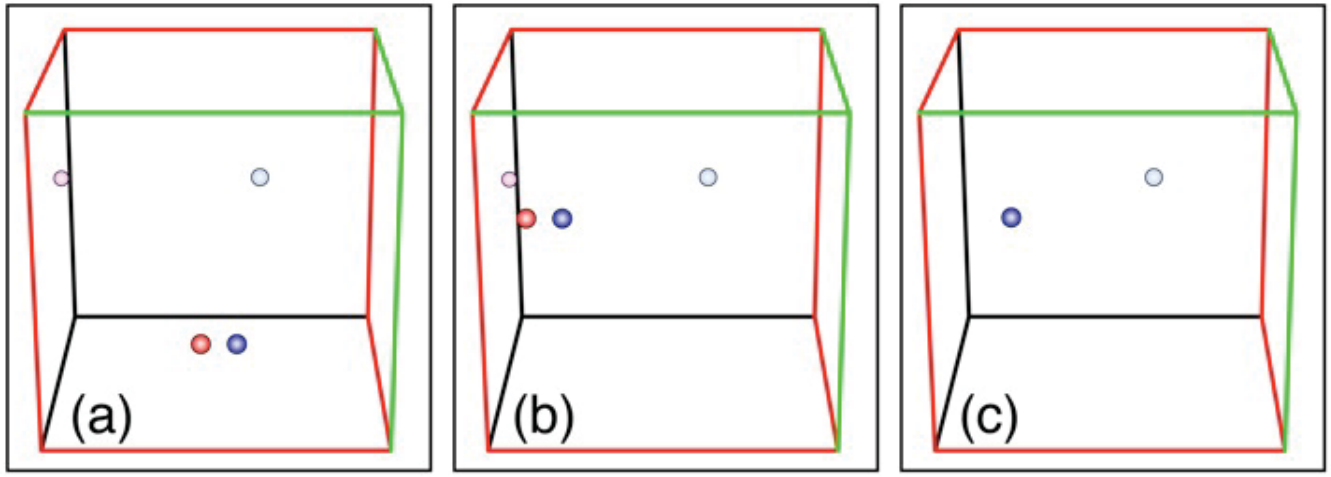

(a) t=0 (b) t=0.081s (c) t=0.081s

The dimer moves as a unit until the O atom recombines. The Mg recombination then quickly follows.

Key: Dark red spheres O interstitials; dark blue spheres Mg interstitials
Light spheres are the vacancies

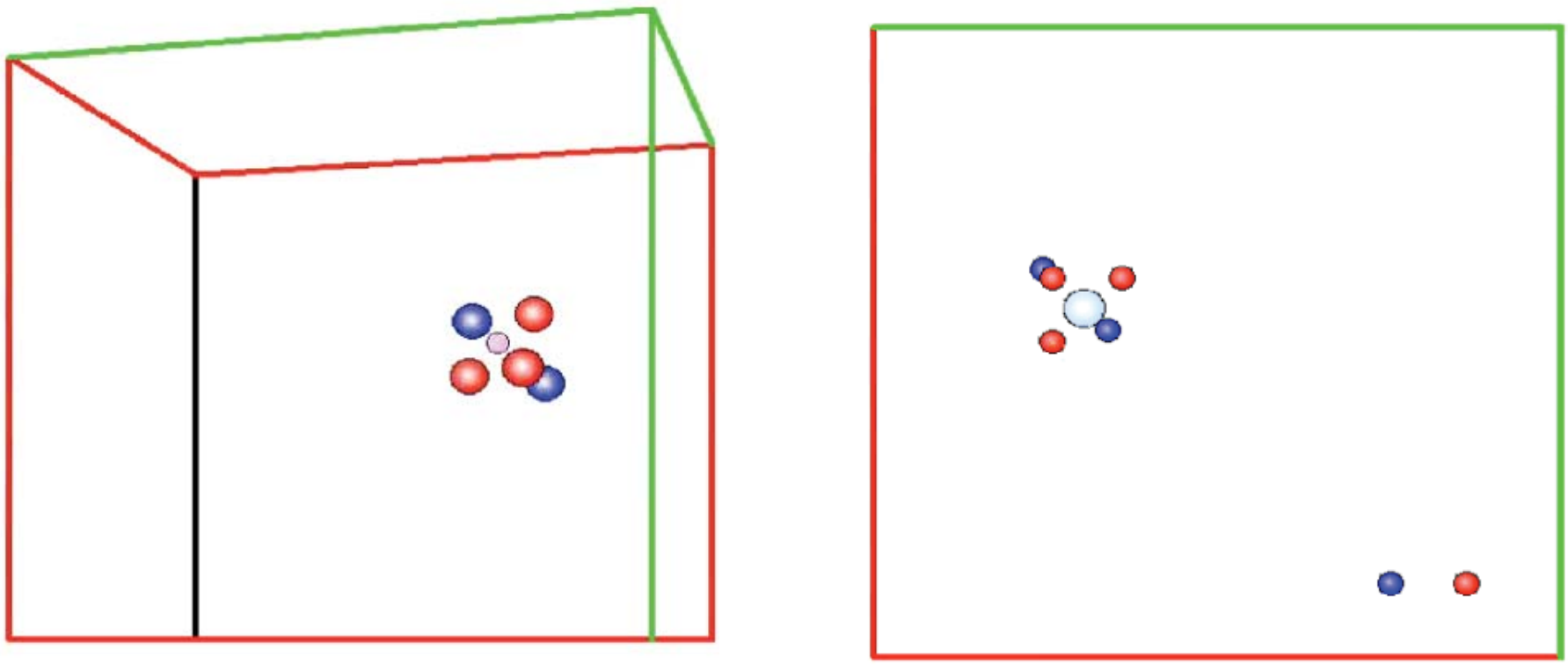

Tetramer diffusion and hexamer formation

Barrier heights and diffusion time scales

No. in cluster	species	barrier (eV)	event time at 300 K (s)	note
1	Mg_i	0.32	10^{-8}	
1	V_{Mg}	2.12	10^{21}	
1	O_i	0.40	10^{-7}	
1	V_O	2.00	10^{21}	
2	$(MgO)_i$	0.75	0.1	
		0.66	0.01	DFT
2	V_{MgO}	2.49	10^{27},	V_O hop,
		0.99	10^3	V_{Mg} catch up
2	V_{MgO}	2.53,	10^{27},	V_{Mg} hop,
		1.03	10^3	V_O catch up
3	$(MgOMg)_i$	0.59	10^{-4}	diffusion
		1.23		rotation
3	$(OMgO)_i$	0.61	10^{-4}	diffusion
		1.27		rotation
4	$(2Mg2O)_i$	1.68	10^{15}	
6	$(3Mg3O)_i$	0.24,	10^{-9}	metastable state
		0.33	10^{-8}	metastable state, DFT
		1.04	100	ground state
8	$(4Mg4O)_i$	0.66	0.01	metastable state
		1.70	10^{15}	ground state

Cluster dynamics: Kinetics of the pentamer cluster in MgO

- Two versions of pentamer:
  - Mg_2O_3
  - Mg_3O_2
- Both can exist in 3 forms
- Each has unique diffusive characteristics
  - A: diffuses quickly in <110> direction
  - B: diffuses more slowly, again in <110> direction
  - C: immobile at 300K
- A, B and C behave similarly for both pentamers
- But decay between forms is different

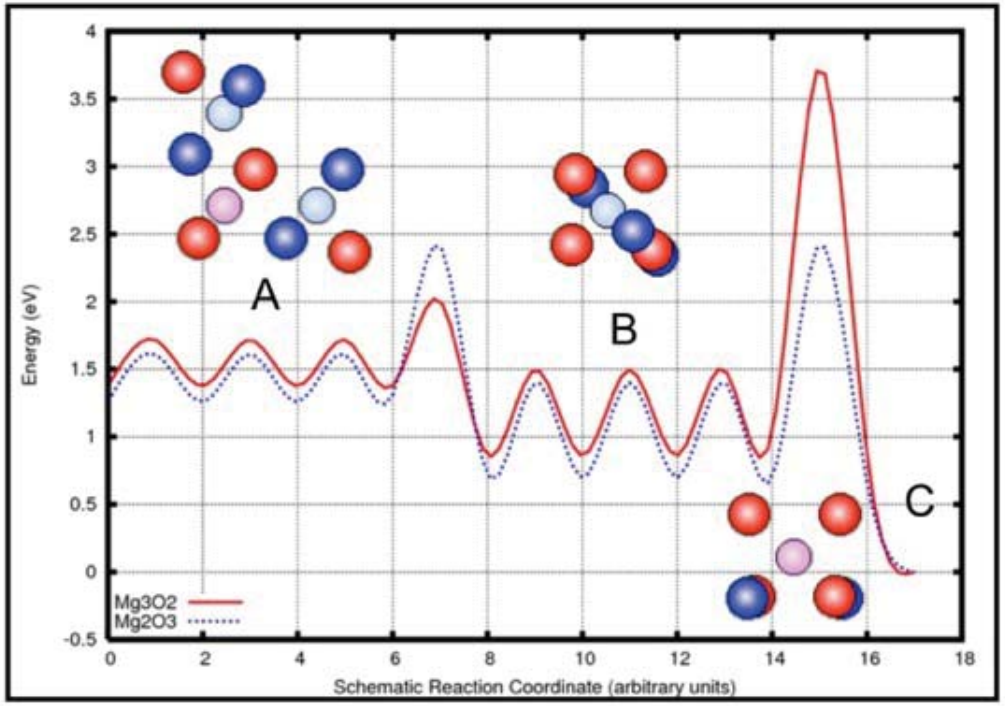

- Encounters of $MgO+MgO_2$ can form any type of Mg_2O_3
  - 10 simulations: 1 forms A, 7 form B, 2 form C

Uberuaga, Smith et al *PRL* **92**, 115505 (2004); *PRB* **72**, (2005); *NIMB* **28**, 260 (2005)

Interstitial cluster kinetics in MgO

- Diffusion barrier of ground state structures follow no clear pattern
- For clusters of size 5 and greater, there are metastable structures that diffuse faster than the ground state

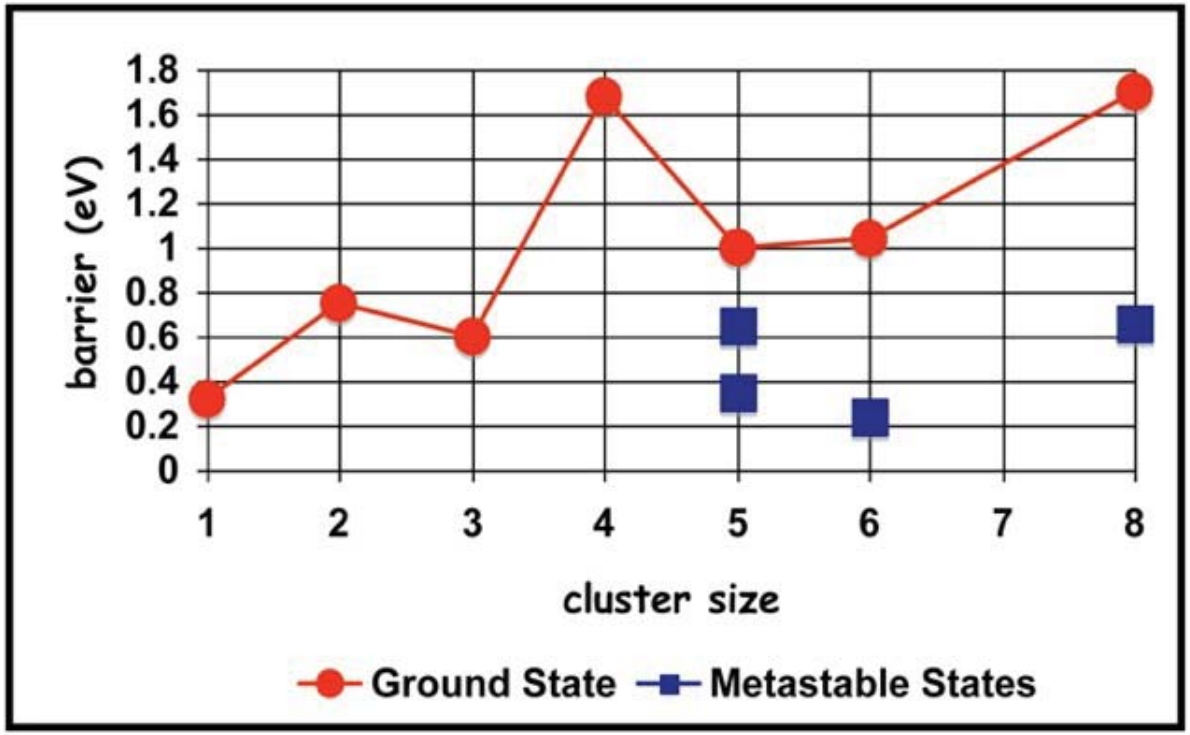

Uberuaga, Smith et al *PRL* **92**, 115505 (2004); *PRB* **72**, (2005); *NIMB* **28**, 260 (2005)

Rate theory example for long time scale effects (radiation damage defect accumulation in MgO)

$$\frac{dC_v}{dt} = (1 - C_v)(1 - Z_1 C_v)P - Z_1 \sum_{n=1}^{n_{max}} \Gamma_{i_n} C_v C_{i_n}, \quad (1)$$

$$\frac{dC_{i_n}}{dt} = (1 - C_v)(1 - Z_1 C_v)P\delta_{n1} + Z_2 \sum_{p=1}^{n-1} \sum_{q \geqslant p}^{n-1} \delta_{n(p+q)}(\Gamma_{i_p} + \Gamma_{i_q}) C_{i_p} C_{i_q} - Z_3 \Gamma_{i_n} \sqrt{C_{iL} C_L} C_{i_n} - Z_1 \Gamma_{i_n} C_v C_{i_n} - Z_2 \sum_{p=1}^{p \leqslant n} (\Gamma_{i_n} + \Gamma_{i_p}) C_{i_n} C_{i_p}, \quad (2)$$

$$\frac{dC_L}{dt} = Z_2 \sum_{p=1}^{n_{max}} \sum_{q \geqslant p}^{n_{max}} \Theta(p + q - n_{max})(\Gamma_{i_p} + \Gamma_{i_q}) C_{i_p} C_{i_q}, \quad (3)$$

$$\frac{dC_{iL}}{dt} = Z_3 \sum_{p=1}^{n_{max}} p \Gamma_{i_p} \sqrt{C_{iL} C_L} C_{i_p} + A \frac{dC_L}{dt}. \quad (4)$$

Dependent variables

C_V- concentration of vacancies
C_{in} - concentration of interstitial clusters of size n
C_L - concentration of interstitial loops
C_{iL} - concentration of interstitials in the above loops

Parameters
P - damage production rate of interstitials and vacancies
Z_1 - capture volume of the vacancies (for interstitials)
Z_2 - capture volume of interstitials with each other
Z_3 - capture volume of interstitial loops with interstitial clusters
n_{max} - largest interstitial cluster size considered. Anything > n_{max} is considered to be a loop
A - average number of interstitials put into new loops when a new loop is formed
Γ_{i_n} - hopping rate of interstitial clusters of size n

See e.g. Yoshida and Kiritani (1973); Uberuaga, Smith et al NIMB (2005)

Effects of cluster mobility on observables

- 1-D reaction rate theory
  - Mobilities from TAD
  - Steady-state conditions
- Size of loops increases by more than 3 times when large clusters are mobile
  - "large" clusters contain more than 1 interstitial
- Enhanced defect mobility results in fewer, larger loops

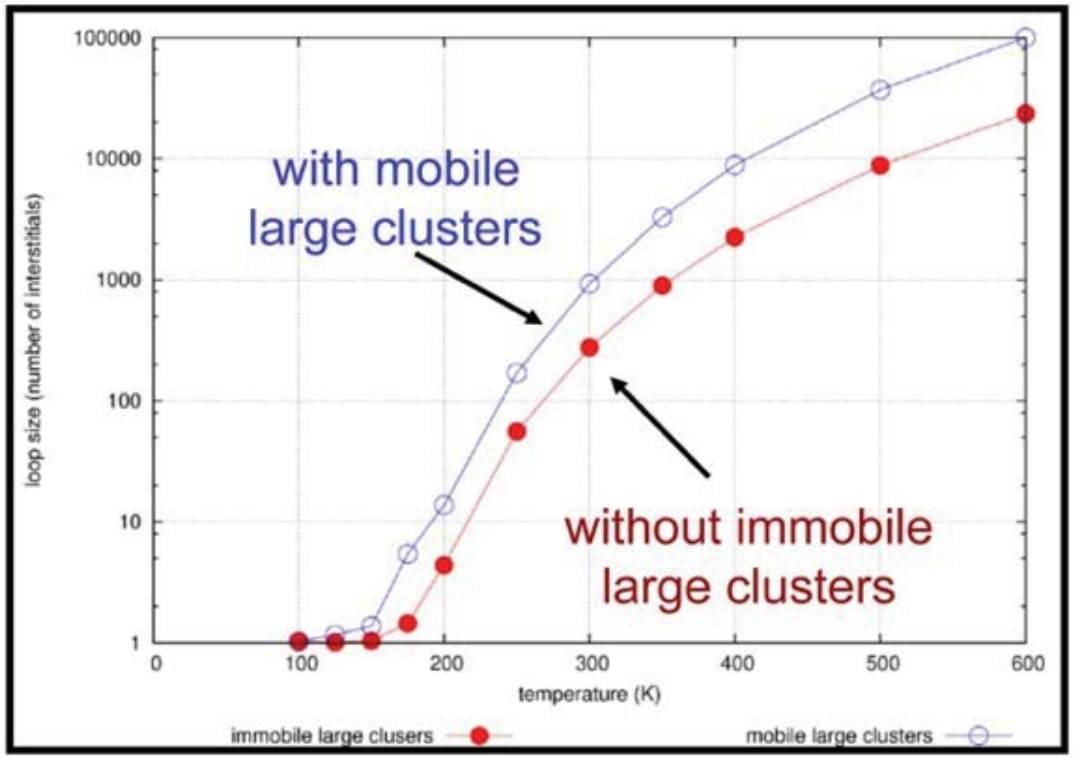

Uberuaga, et. al., *PRL* **92**, 115505 (2004); *PRB* **72**, (2005); *NIMB* **28**, 260 (2005)

Long time scale dynamics required because it showed the aggregation of interstitials into clusters lead to metastable clusters with high mobility

The lifetime of clusters would be missed if only high temperature simulations were carried out.

MD simulations of radiation effects in spinels

Spinel Structures

Close-packed O^{2-} structure

Site type	Total	$MgAl_2O_4$	$MgGa_2O_4$	$MgIn_2O_4$
		Mg^{2+}/Al^{3+} *i=0*	Mg^{2+}/Ga^{3+} *i=0.5*	Mg^{2+}/In^{3+} *i=1*
Tetrahedral 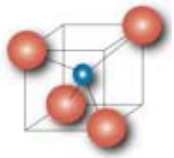	64	8/0	4/4	0/8
Octahedral 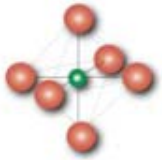	32	0/16	4/12	8/8
		normal	disordered	inverse

 Oxygen

Molecular Dynamics Setup

- Collision cascades were performed in
  - $MgAl_2O_4$ normal spinel (i = 0)
  - $MgGa_2O_4$ disordered spinel (i=0.5)
  - $MgIn_2O_4$ inverse spinel (i = 1)
- PKA energy: 0.4 - 10 keV, up to 1 million atoms
- Ionic interactions: Buckingham potential
- Fast multipole method for electrostatic computation without PBC
- Atoms embedded in a charge neutral cell
- Initial temperature of 0 K, runtime of ~ 10 ps

Loughborough University

0.4 keV spinel cascade snapshots

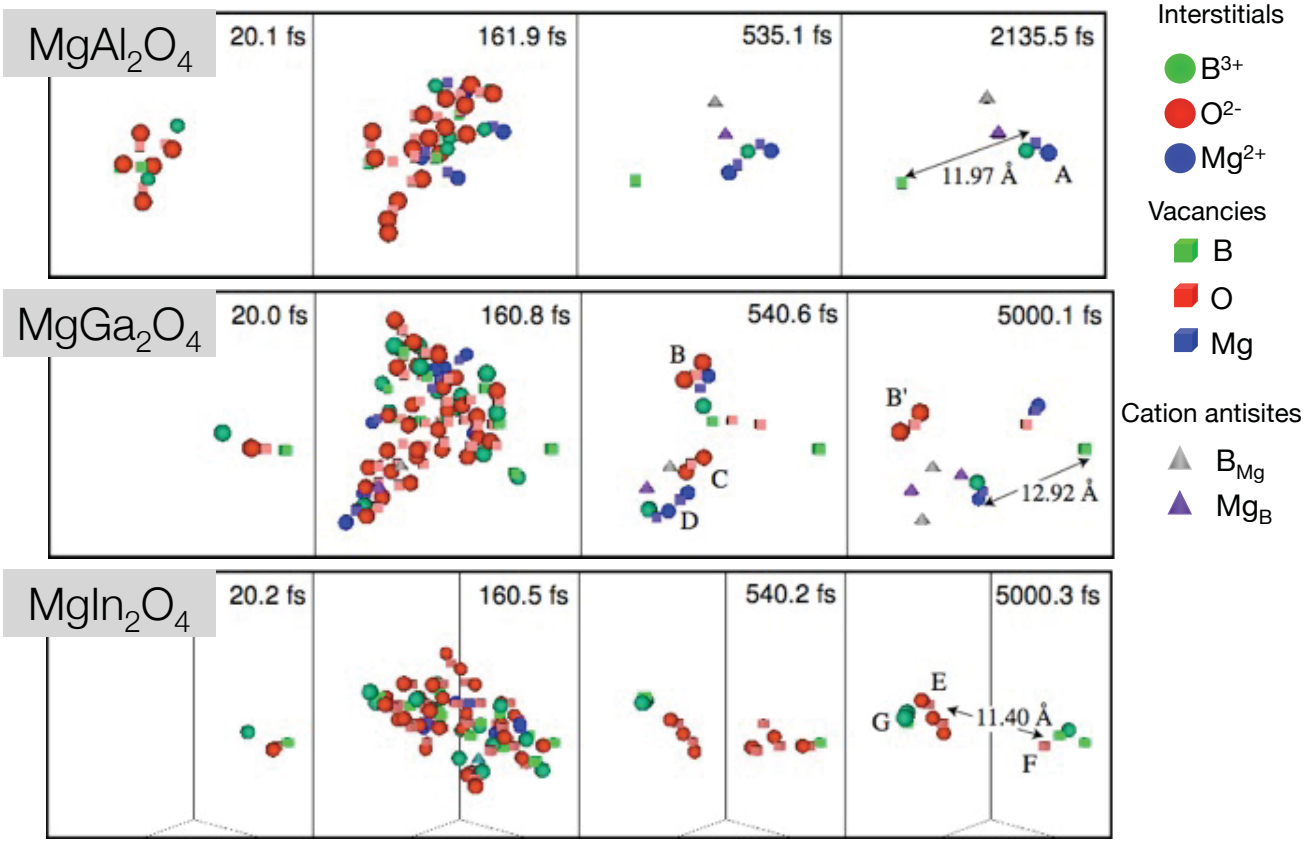

2 keV damage in spinels

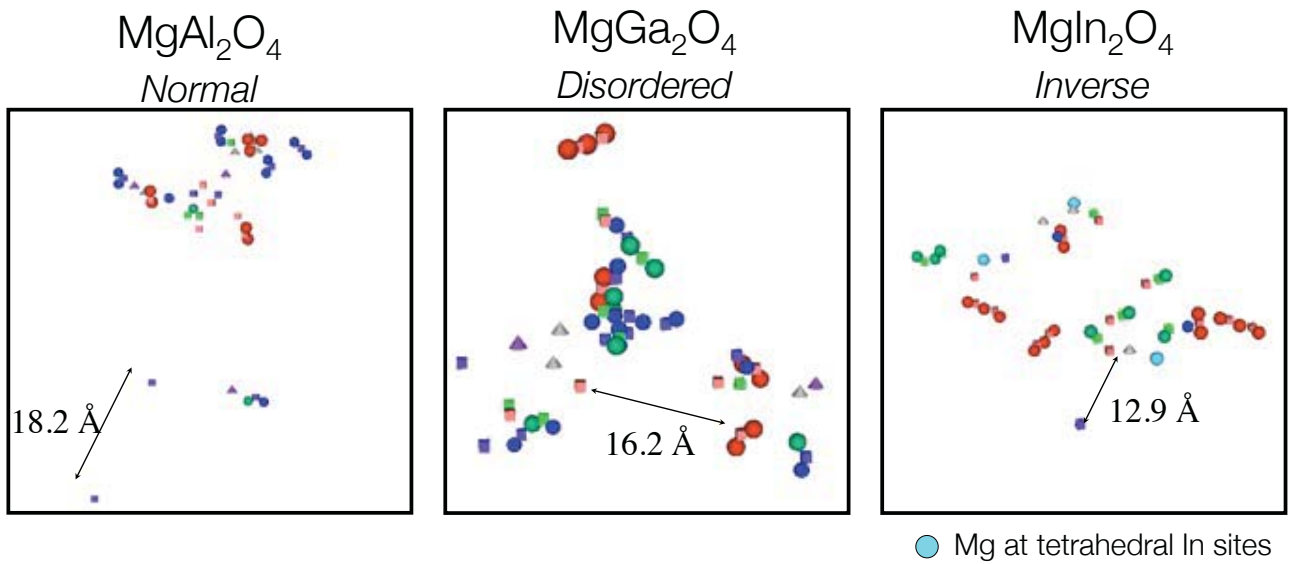

Cascades more compact in disordered and inverse spinels

$MgGa_2O_4$: interstitial - vacancy recombination difficult

5 keV cascades set up by B^{3+} ions

$MgAl_2O_4$ | $MgGa_2O_4$ | $MgIn_2O_4$

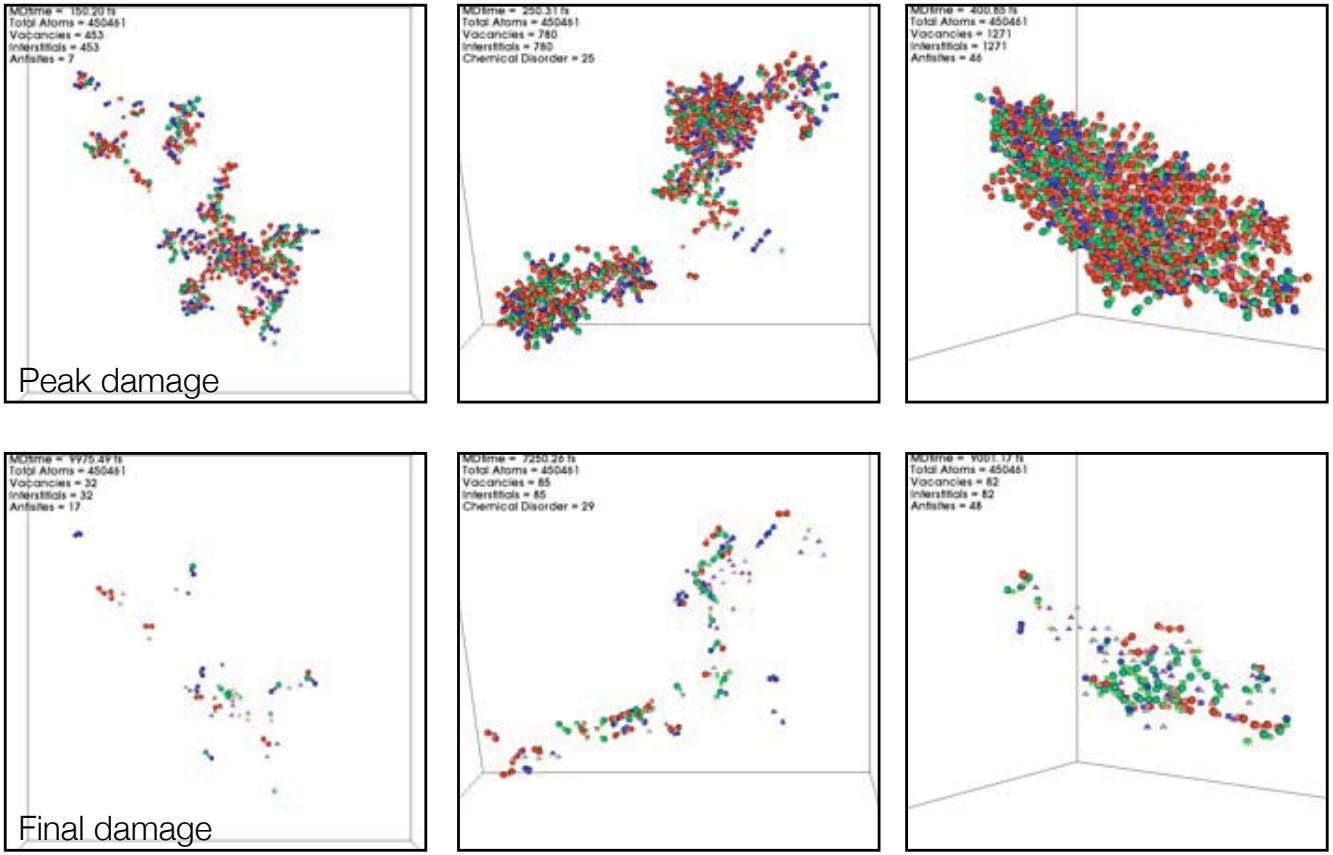

10 keV cascade in normal spinel

Interstitials

- Al^{3+}
- O^{2-}
- Mg^{2+}

Vacancies

- Al
- O
- Mg

Cation antisites

- Al_{Mg}
- Mg_{Al}

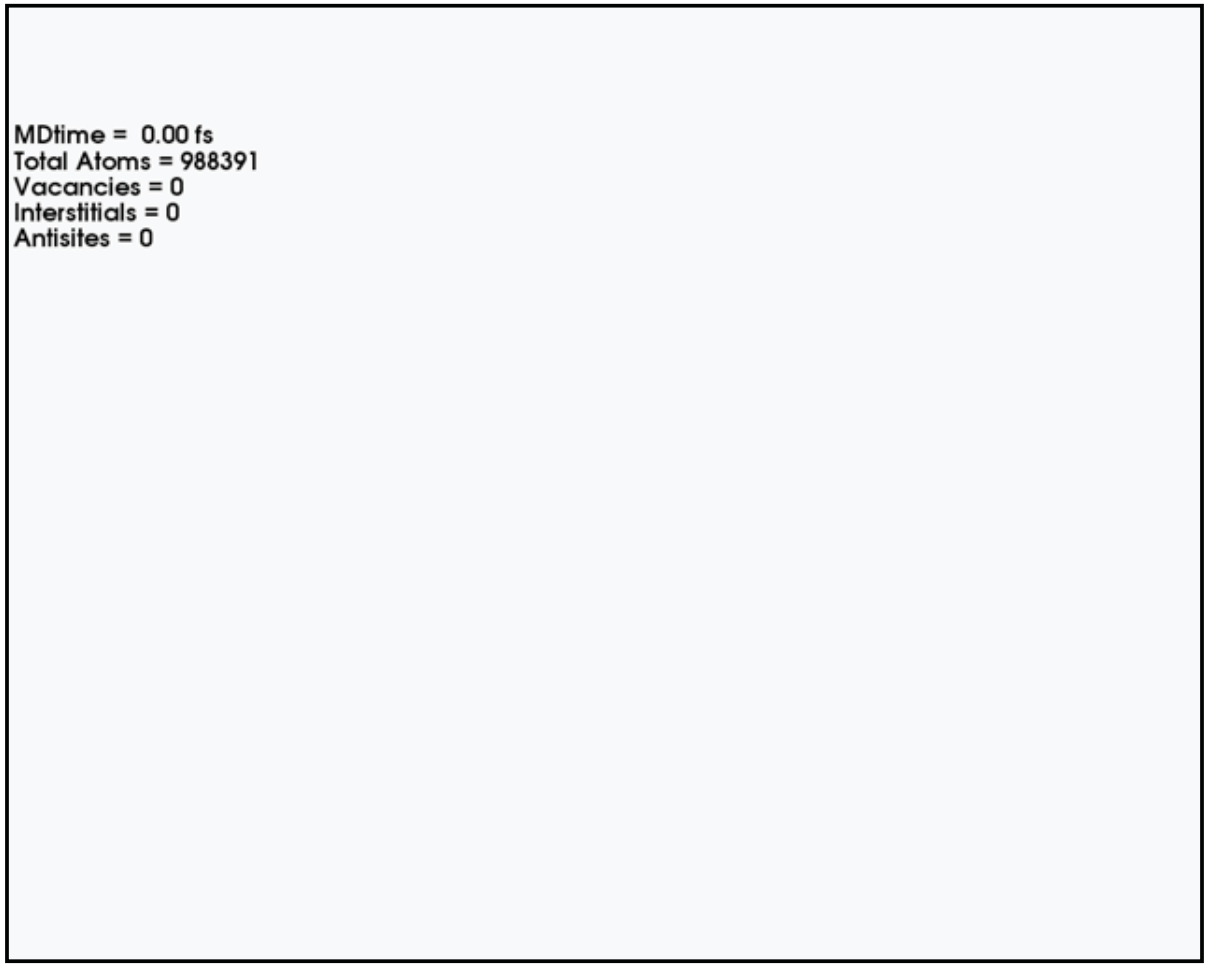

Loughborough University

Defects in normal spinel, $MgAl_2O_4$

Perfect structure

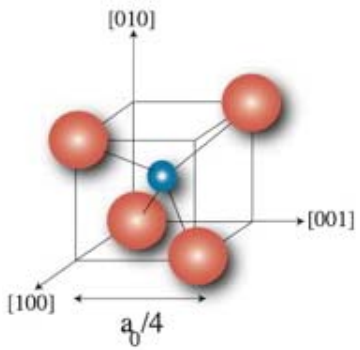

Cation split interstitial

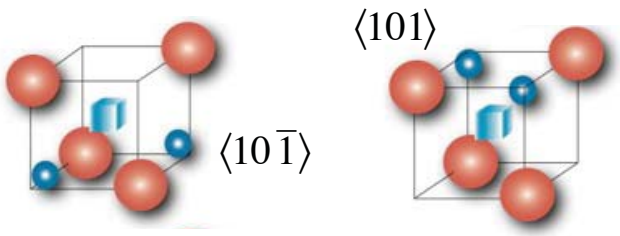

Anion split interstitial

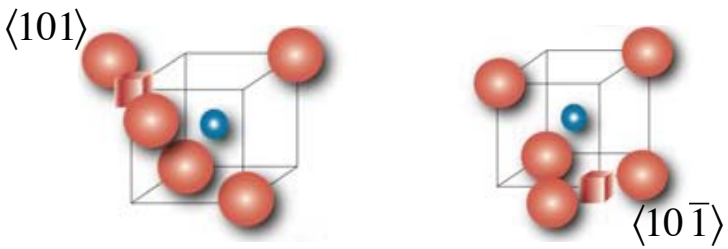

Point defect diffusion in normal spinel, $MgAl_2O_4$

	Defect	Barrier, E_a (eV)	Mechanism
1*	O_i	0.29 0.64, 0.67	1-D along <110> diffuses to new <110> row
2*	Mg_i	0.56, 0.74	3-D
3**	Al_i	N/a 0.57	Forms Mg-Al cation split Al antisite + Mg_i
4	V_{Mg}	0.68	3-D
5	V_O	1.49, 1.66	3-D
6	V_{Al}	2.00	3-D

* Mechanisms depicted during interstitial-vacancy recombination in the collision cascades

** Al_i defect formed Mg-Al split interstitials during the collision cascades before the Al decays to an antisite +Mg interstitial

Diffusion in normal spinel, $MgAl_2O_4$ using TAD

E_a = 0.29 eV

t = ns

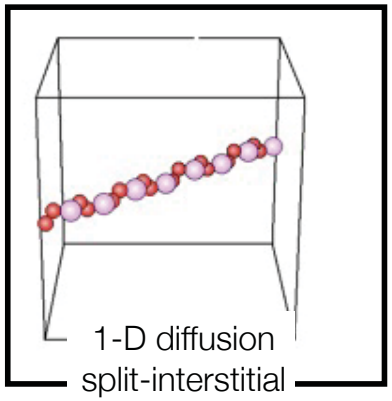

E_a = 0.56 eV

t = ms

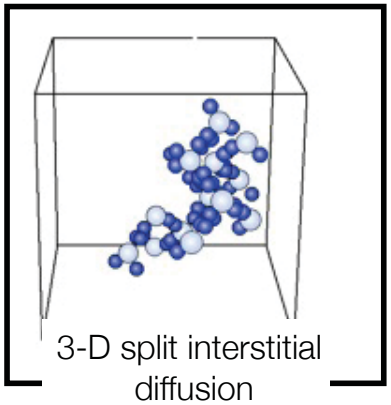

O vacancy O interstitial

Mg vacancy Mg interstitial

E_a = 1.49 eV

t = 10^{12} s

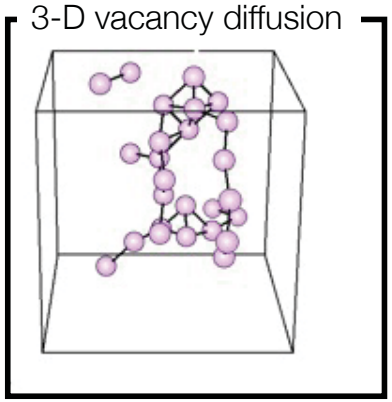

E_a = 0.68 eV

t = ms

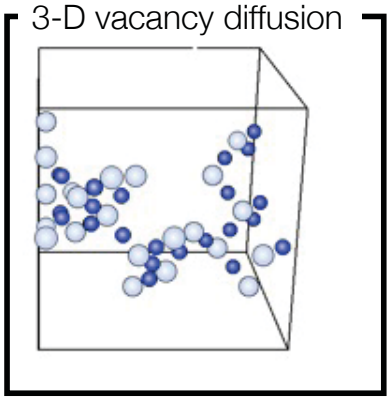

Defect motion in disordered $MgGa_2O_4$

	Defect	Barrier (eV)	Mechanism
1	O_i	0.09 - 0.89 0.51 - 0.99	1-D along <110> 3-D on O sublattice
2	Mg_i	0.15 - 0.69	3-D
3	Ga_i	0.23	Ga antisite + Mg_i
4	V_{Mg}	0.18 - 1.07	3-D
5	V_O	0.59 - 0.85	3-D from Ga rich to Mg rich
6	V_{Ga}	0.63	Mg antisite + V_{Mg}

- Range of energies for defect motion
- Diffusion restricted to a few sites where the defects are trapped
- O vacancy starting with 4 Ga nearest neighbours ends up in Mg rich region
- Ga defects form Mg defects

Defect motion in disordered $MgGa_2O_4$

Complex electrostatic field due to disorder results in different vacancy site energies

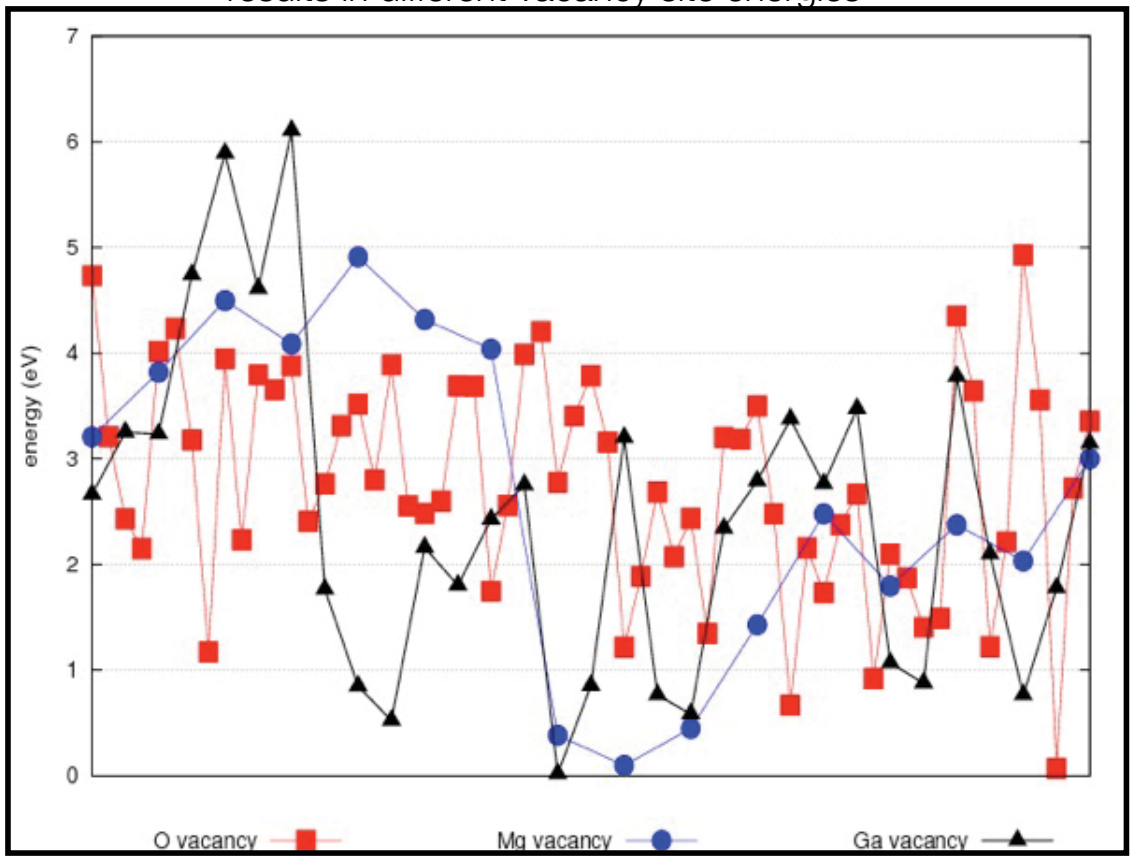

Defect motion in the inverse $MgIn_2O_4$

	Defect	Barrier (eV)	Mechanism
1	O_i (crowdion)	0.32, 0.89 0.80 - 1.33	1-D along <110> Re-orients to <110>
2	Mg_i	N/a	Forms Mg-In split interstitial
3*	In_i (split)	0.07 0.11 - 0.60	Forms **crowdion**‡ defect Crowdion to crowdion hops
4	V_{Mg}	1.02 - 1.12	3-D on Mg sublattice
5	V_O	0.60 - 1.36	3-D
6	V_{In} (Tetra)	0.23	In **split vacancy**‡ defect
7	V_{In} (Octa)	1.24, 1.34	Mg antisite + V_{Mg}

* One of the main defects from the collision cascades

‡ In_i residing at octahedral interstice

Loughborough University

Defect motion in the inverse $MgIn_2O_4$

1-D O crowdion hops

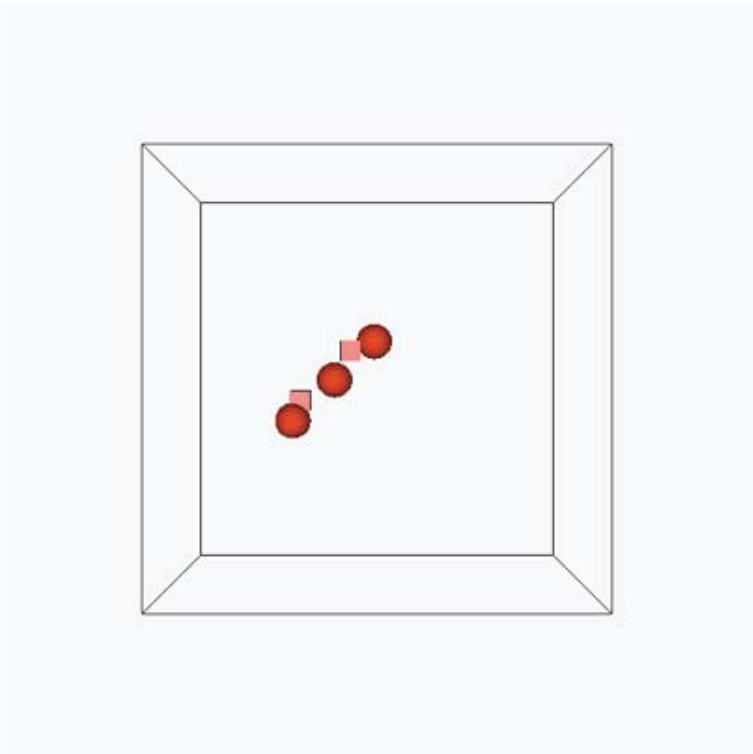

3-D In crowdion hops

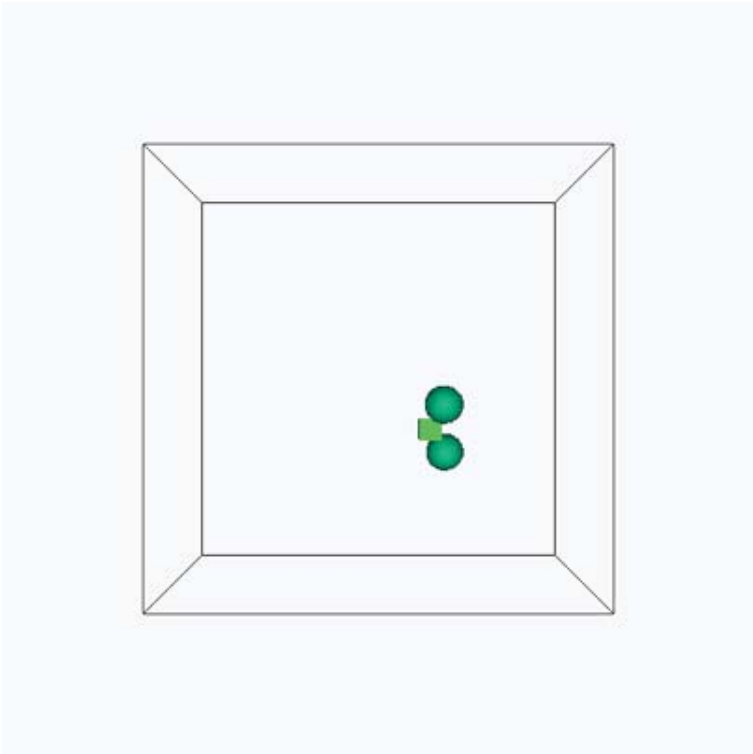

TAD simulations reached the μs timescale

Loughborough University

Steels with embedded nanoparticles (ODS)

Another MD example : Yttria nanoparticles in bcc Fe (ODS)

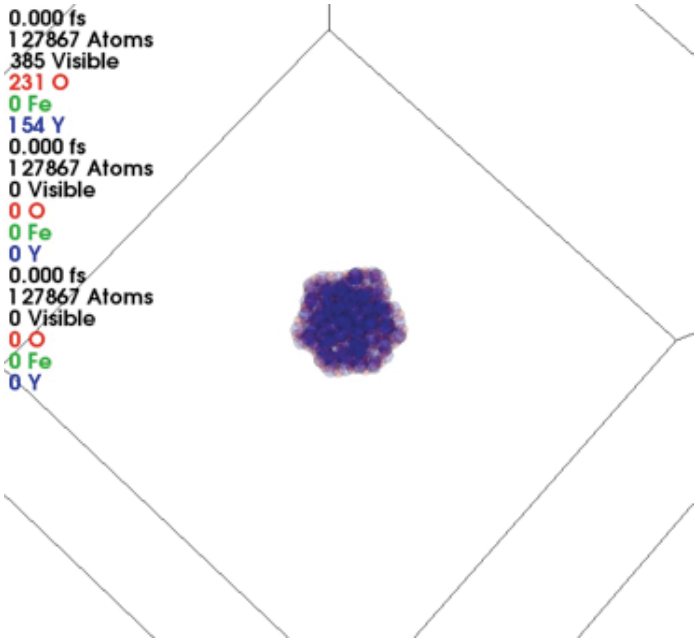

Nanoparticle temperature

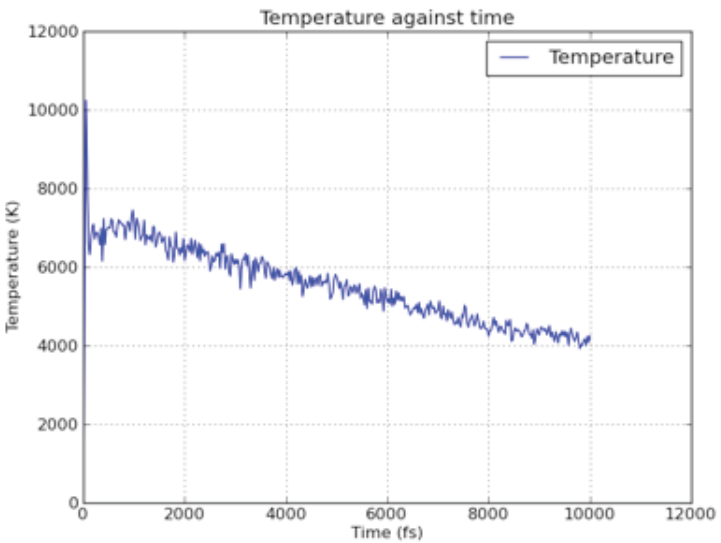

The nanoparticle releases energy over ~50 ps time scale

I keV cascade initiated close to the nanoparticle, showing defect trapping at the interface

Magnetron sputtering and ion beam assist applications of multi-time scale modelling

- TiO_2 and ZnO thin film deposition

Evaporation deposition : assume particles arrive at 1 eV

Magnetron sputtering : assume particles arrive with higher energy, typically 40 eV

We can also vary the fluence to simulate HIPIMS or pulsed DC sputtering and can also vary the energy and stoichiometry of the arriving particles

OTF-KMC for modelling deposition by magnetron sputtering

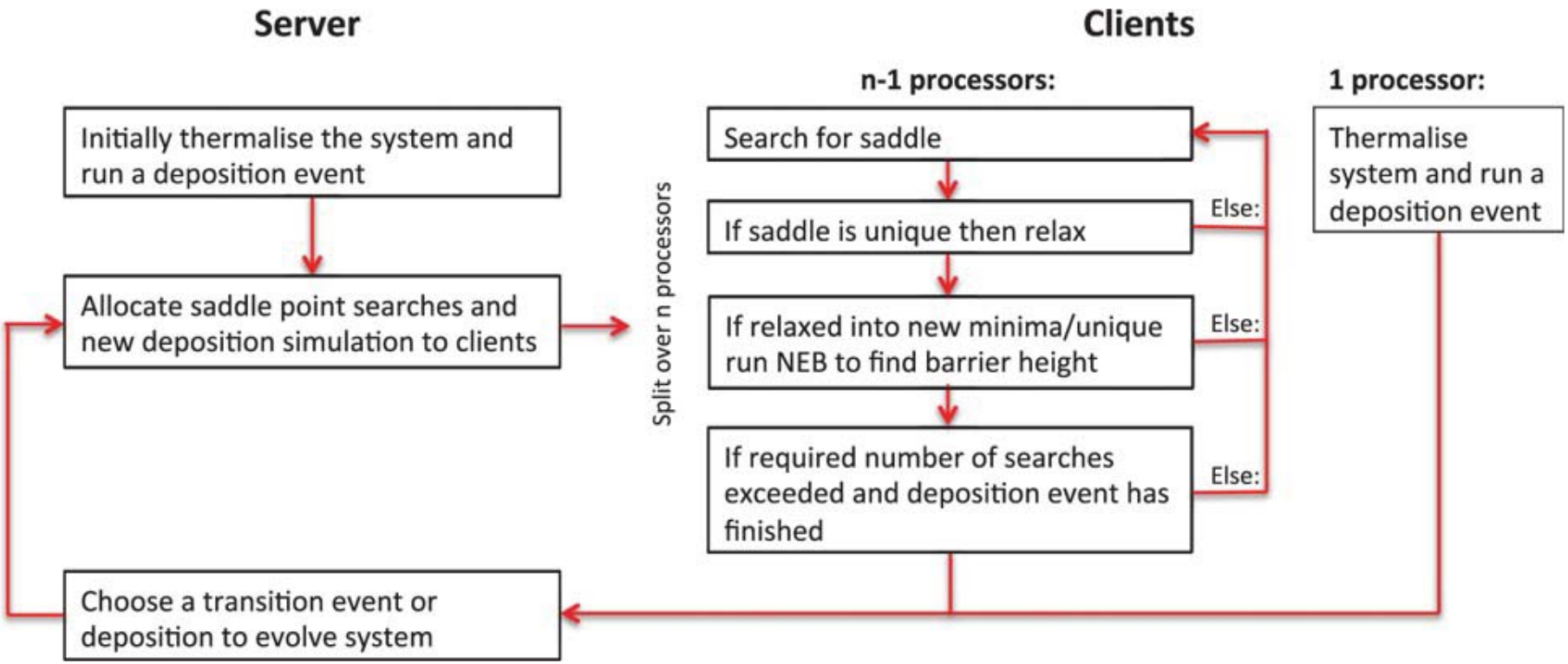

Code is written in Python and wraps around standard MD packages. In our case LBOMD and LAMMPS. The code was developed by Louis Vernon now at LANL and other PhD students in the group

Modelling TiO_2 growth

- Variable charge potential by Hallil et al
- Clean, smooth rutile 1536 atom lattice with 8 layers
- Periodic boundary conditions used, with bottom layer fixed and next layer thermalized, rest of lattice free
- O, O_2, Ti, TiO and TiO_2 clusters are deposited at correct stoichiometry

Main identified mechanisms for TiO_2 growth under low energy impact

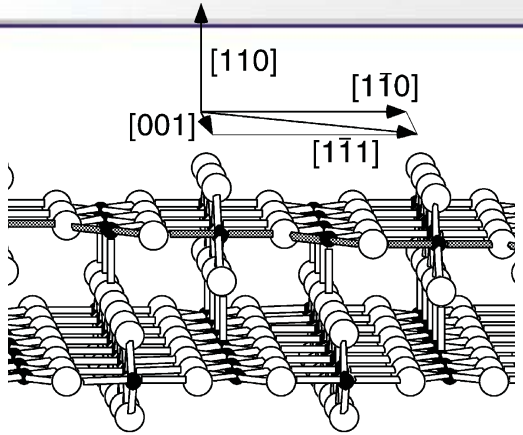

Ti atoms implant below the surface

Almost all O atoms stick on the surface or reflect

O atoms undergo (mainly 1-D) diffusion on the surface

The presence of O adatoms on the surface lowers the energy barriers for the interstitial Ti to diffuse towards the surface thus forming the new TiO_2 units.

Modelling TiO_2 growth

- 40 eV depositions at 350K, simulates sputter deposition at experimental rates of 0.5 mL/s !!
- 4 monolayers of atoms added to rutile {110}
- ~ 6 s simulated

  -using MD only, this would take thousands of years to simulate

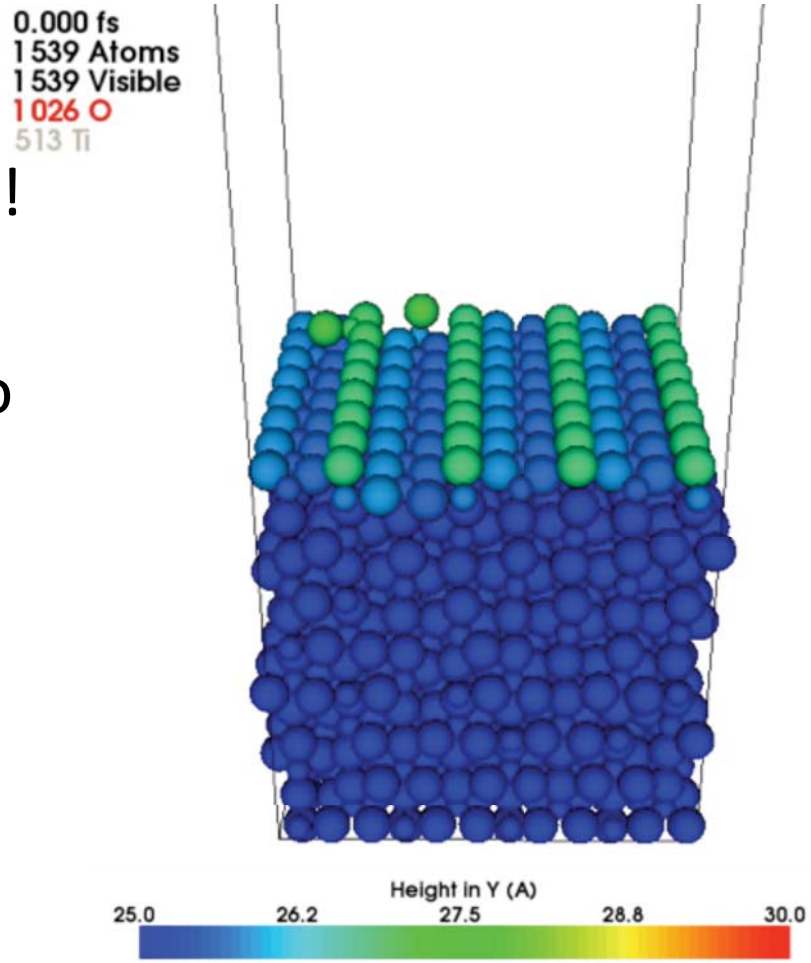

Modelling TiO_2 growth

1 eV ..evaporation process:

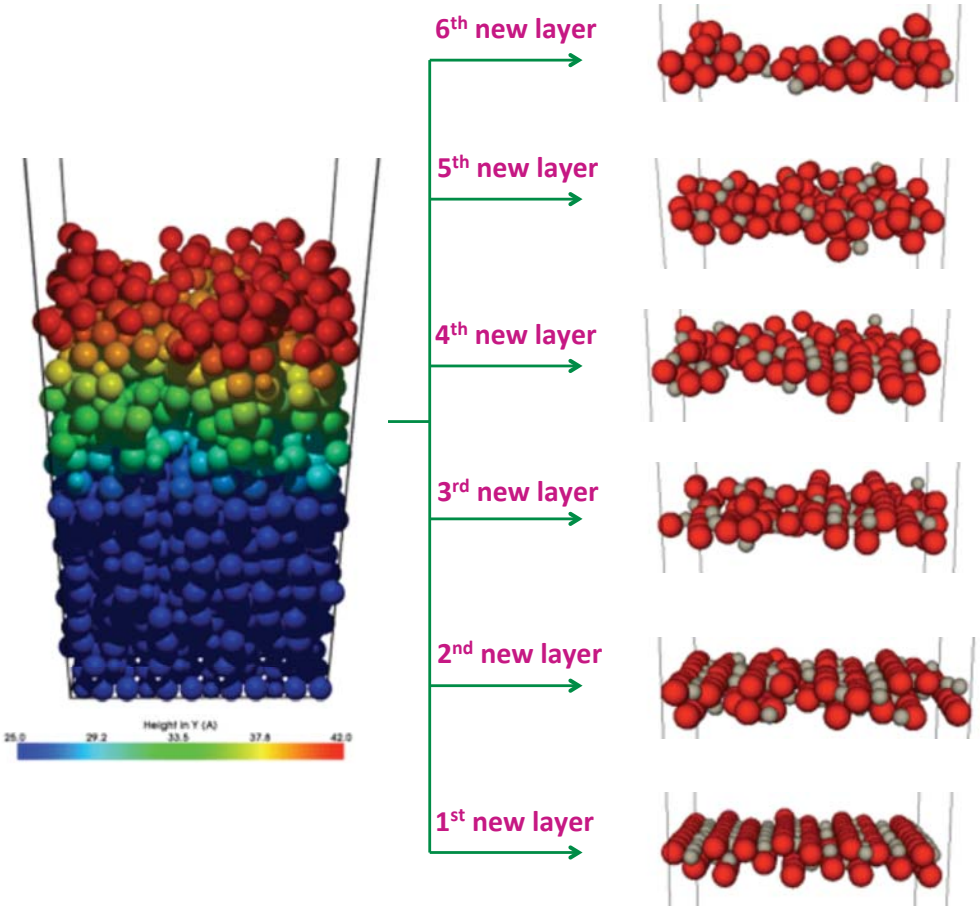

- Atoms missing from layers
- Low energy allows little diffusion
- Little mixing of original atoms

Ti:

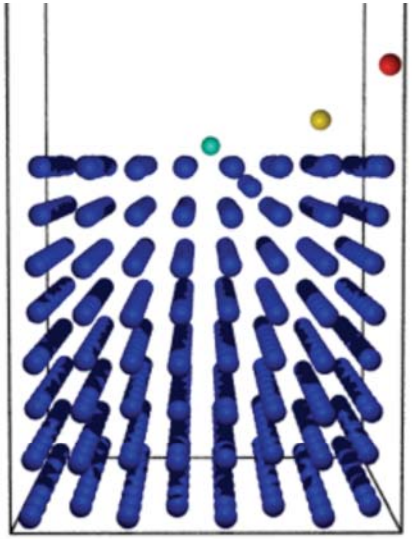

Modelling TiO_2 growth

40eV.. sputter deposition:

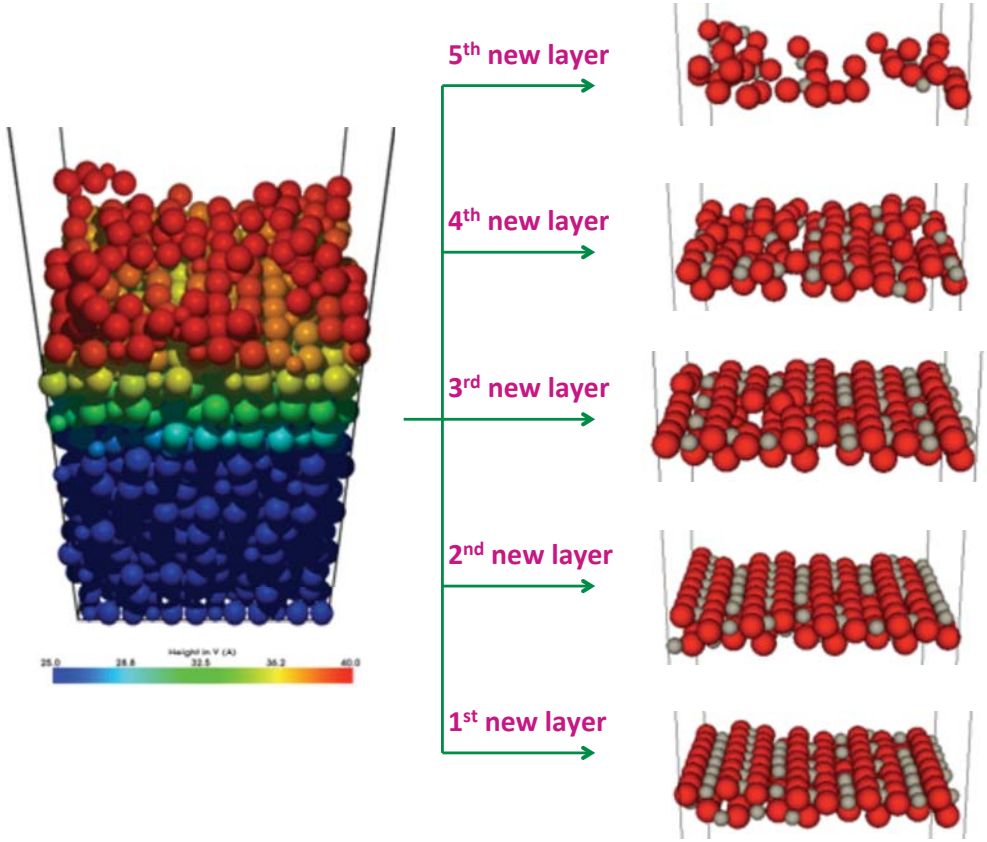

- 3 very good layers
- Mixing mechanism with original substrate, allowing rutile growth mechanism

Ti:

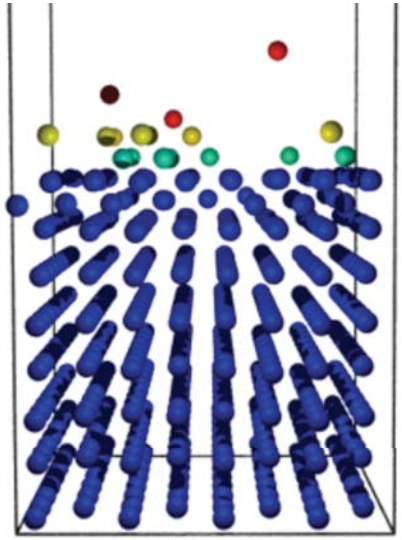

Findings from the TiO_2 simulations

- The main growth mechanisms are identified
- Best crystallinity is obtained with 40 eV bombardment (or with Ar assist at 40 eV) and with an O rich mixture
- If there is too much O in the mixture then the surface etches rather than grows

Modelling ZnO growth

- Variable charge potential ReaXFF (Van Duin)
- Clean, initial smooth wurzite (000-1), 1024 atom lattice with 8 layers
- Periodic boundary conditions used, with bottom layer fixed and the next layer thermalised; rest of lattice free
- O, O_2, Zn and ZnO clusters are deposited with variable mixturesy

Example of an complex transition which cannot be guessed : String vibration on a ZnO surface

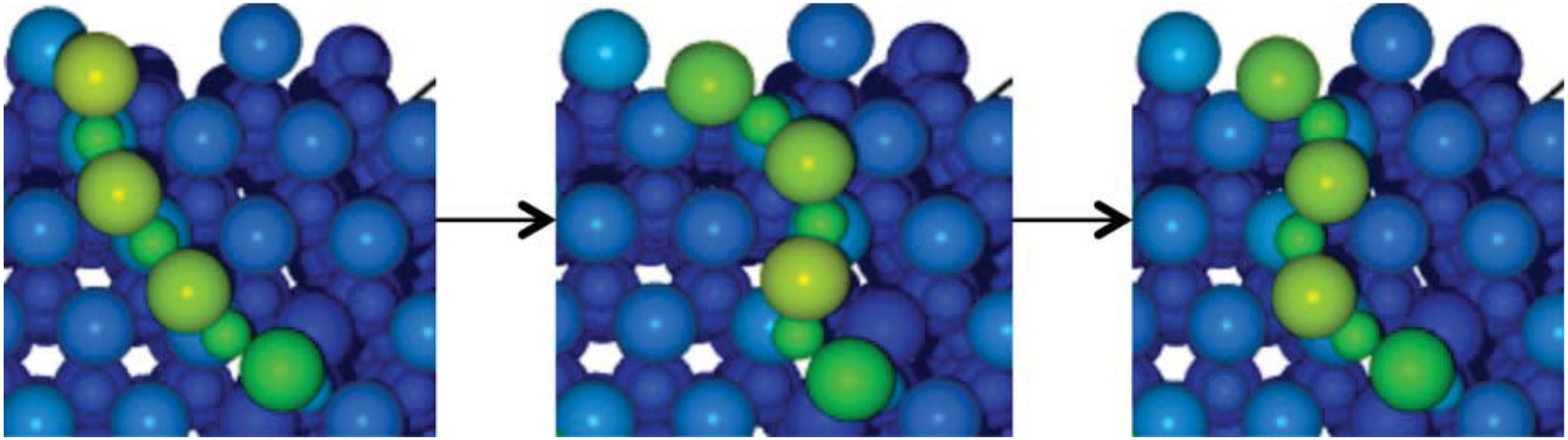

Small spheres represent Zn, large spheres O atoms

ZnO strings form on the surface and move with barriers of around 0.3eV.
When interacting with other such strings they snap into the hexagonal structures to form the crystalline layer

40 eV sequential deposition of Zn_xO_y

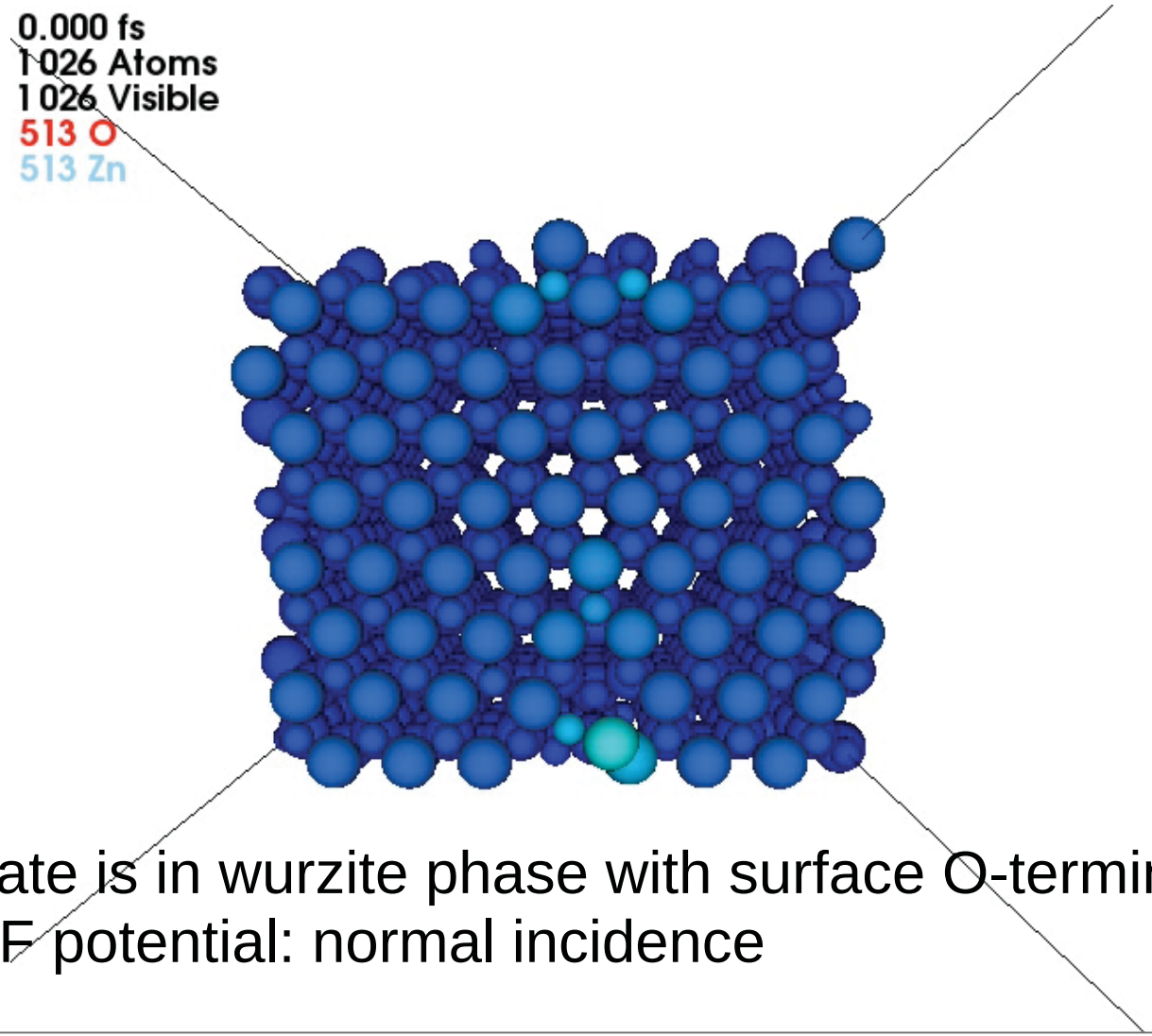

Substrate is in wurzite phase with surface O-terminated
ReaxFF potential: normal incidence

ZnO Evaporation deposition pre-annealing

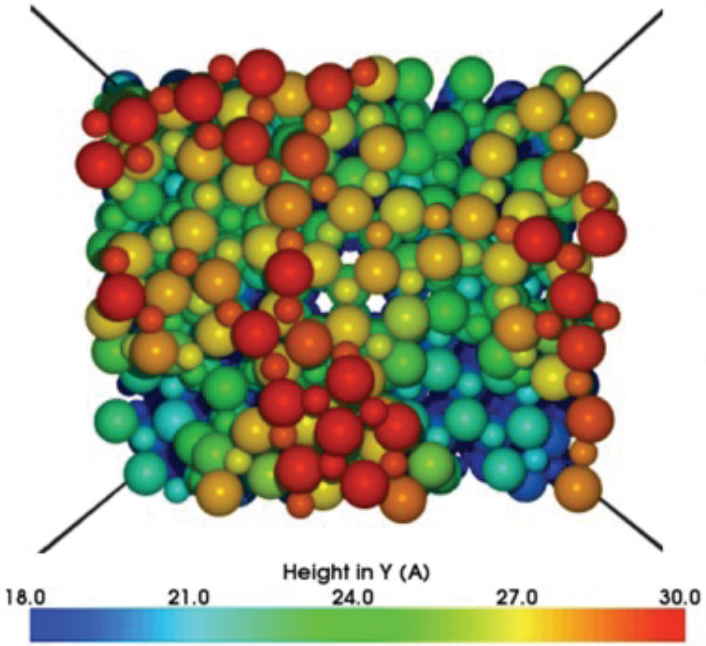

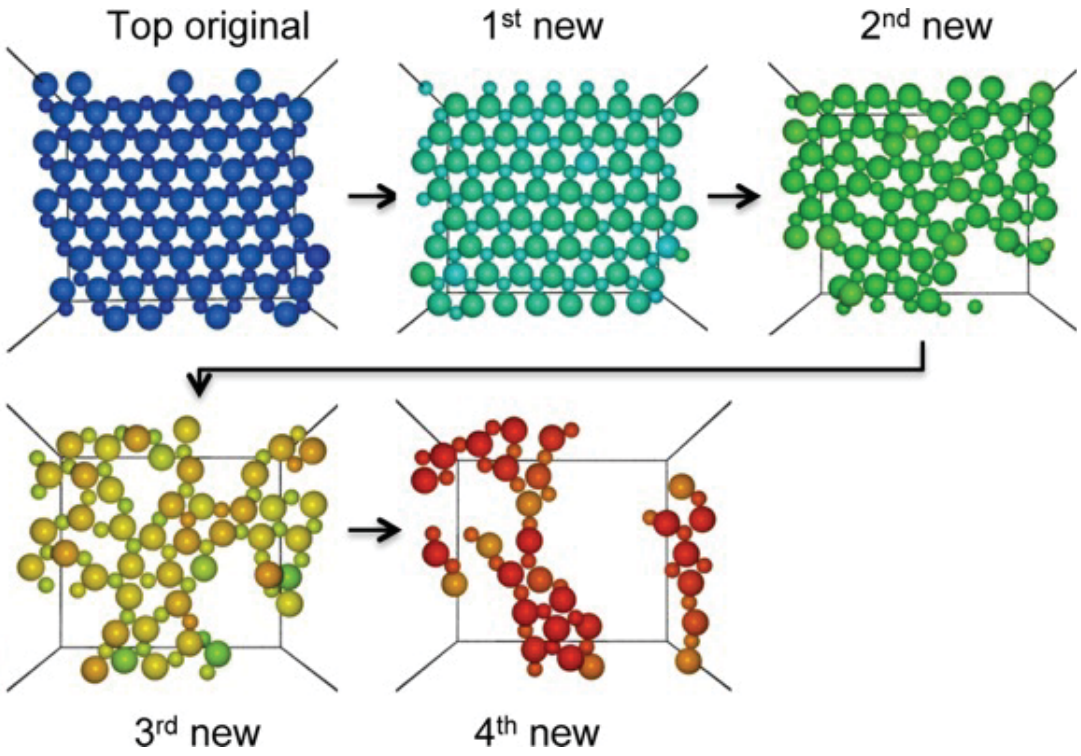

Twin boundary formation (wurzite-zinc blende) after deposition at 40 eV and annealing at 923K

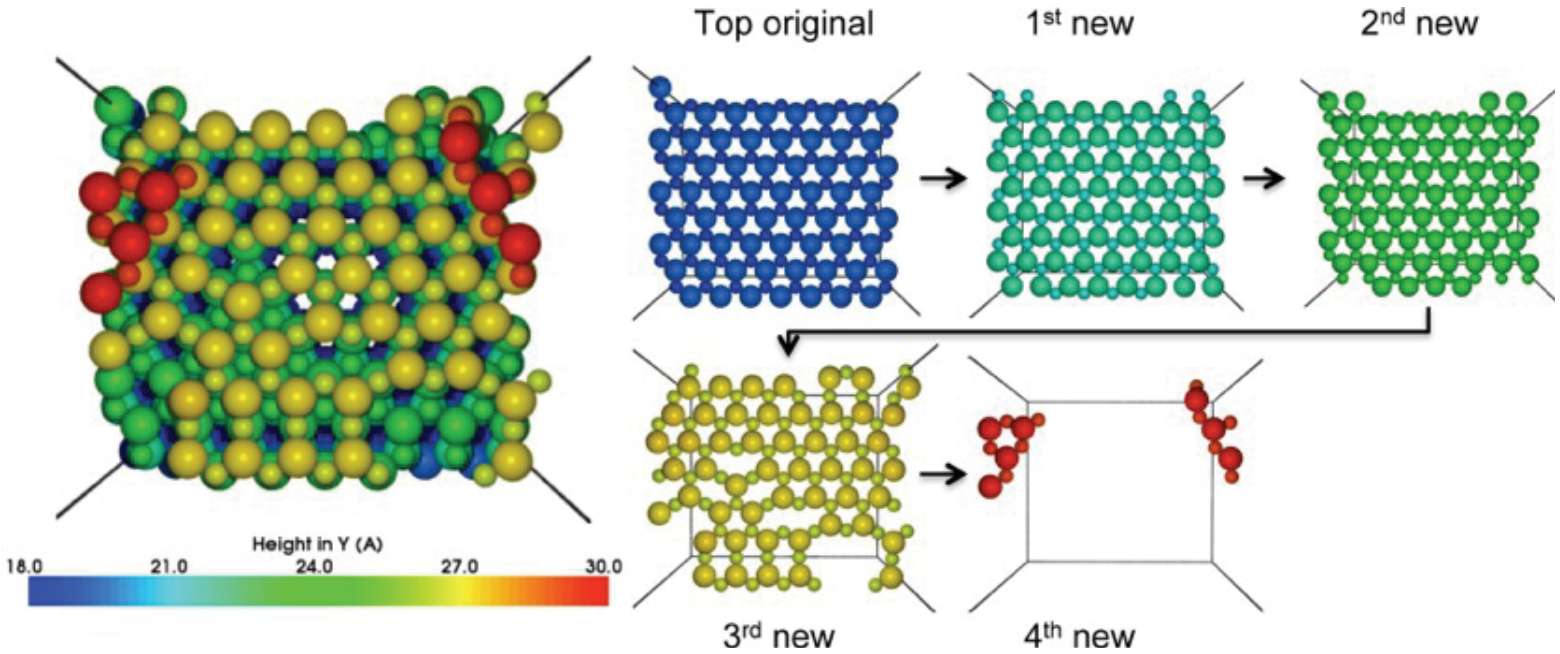

Green circles are O vacancies

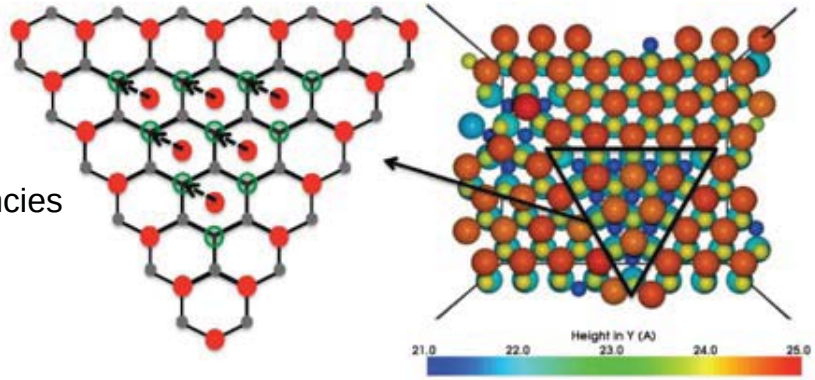

Conclusions from the ZnO simulations

- Twinning can form during the deposition process due to the energetically close wurzite and zinc blende phases
- Strings of atoms form during deposition which lock into place to form teh hexagonal structures
- Heating for a short time (10 ns at 900 K) at high temperatures anneals out the defects.

General Conclusions and Outlook

- Atomistic long time scale techniques can now model ion beam interactions with surfaces, PVD and magnetron sputtering

- Typical reactor radiation dose rates are lower than ion beams but are also beginning to be accessible by the methods

- It would be nice to apply the methods to nuclear waste encapsulation in glasses to predict the behaviour over 100's of years